

Article

MIMO Relaying UAVs Operating in Public Safety Scenarios

Joseanne Viana ^{1,2,*}, Francisco Cercas ^{1,2}, Américo Correia ^{1,2}, Rui Dinis ^{2,3} and Pedro Sebastião ^{1,2}

¹ Radio Systems Department, ISCTE—Instituto Universitário de Lisboa, Av. das Forças Armadas, 1649-026 Lisbon, Portugal; francisco.cercas@iscte.pt (F.C.); americo.correia@iscte-iul.pt (A.C.); pedro.sebastiao@iscte-iul.pt (P.S.)

² IT—Instituto de Telecomunicações, Av. Rovisco Pais, 1, Torre Norte, Piso 10, 1049-001 Lisboa, Portugal; rdinis@fct.unl.pt

³ FCT—Universidade NOVA de Lisboa, Monte da Caparica, 2829-516 Caparica, Portugal

* Correspondence: joseanne.viana@lx.it.pt

Abstract: Methods to implement communication in natural and humanmade disasters have been widely discussed in the scientific community. Scientists believe that unmanned aerial vehicles (UAVs) relays will play a critical role in 5G public safety communications (PSC) due to their technical superiority. They have several significant advantages: a high degree of mobility, flexibility, exceptional line of sight, and real-time adaptative planning. For instance, cell edge coverage could be extended using relay UAVs. This paper summarizes the sidelink evolution in the 3GPP standardization associated with the usage of the device to device (D2D) techniques that use long term evolution (LTE) communication systems, potential extensions for 5G, and a study on the impact of circular mobility on relay UAVs using the software network simulator 3 (NS3). In this simulation, the transmitted packet percentage was evaluated where the speed of the UAV for users was changed. This paper also examines the multi-input multi-output (MIMO) communication applied to drones and proposes a new trajectory to assist users experiencing unfortunate circumstances. The overall communication is highly dependent on the drone speed and the use of MIMO and suitable antennas may influence overall transmission between users and the UAVs relay. When the UAVs relaying speed was configured at 108 km/h the total transmission rate was reduced to 55% in the group with 6 users allocated to each drone.

Keywords: UAV; drones; disasters; relaying; 4G; 5G; drone simulation; sidelink; NS3; MIMO



Citation: Viana, J.; Cercas, F.; Correia, A.; Dinis, R.; Sebastião, P. MIMO Relaying UAVs Operating in Public Safety Scenarios. *Drones* **2021**, *5*, 32. <https://doi.org/10.3390/drones5020032>

Academic Editor:
Abderrahmane Lakas

Received: 15 March 2021
Accepted: 22 April 2021
Published: 26 April 2021

Publisher's Note: MDPI stays neutral with regard to jurisdictional claims in published maps and institutional affiliations.



Copyright: © 2021 by the authors. Licensee MDPI, Basel, Switzerland. This article is an open access article distributed under the terms and conditions of the Creative Commons Attribution (CC BY) license (<https://creativecommons.org/licenses/by/4.0/>).

1. Introduction

Public safety communication services often utilize unmanned aerial vehicles (UAVs) as a suitable tool during unfortunate events such as landslides, mountain collapses, and road accidents due to the full line of sight (LoS) probability when flying above a given height as the 3GPP Release 15 presents [1,2]. UAVs show superiority in comparison to existing terrestrial base stations in terms of convenient deployment for covering dead zones, easy control, coverage area adaptation, and flexibility in network reconfiguration [3]. These advantages made the European Union constitute the U-Space program to legislate UAV's integration into their aircraft system. The program objective established commercial management rules for UAVs in Europe [4]. According to Bekkouche et al. [5], UAVs can contribute to enhancing user services in heterogeneous radio access networks (RANs) as a relay (Figure 1), as Wi-Fi connected to a backhaul, as a small cell and/or base station to provide coverage extension, and as storage in delay tolerant networks for late forwarding.

Indeed, drones' major user contract application is as a relay because of the costly considerations and licenses for fixed relay implementations that avoid obstacles and complex topographical regions [6]. Additionally, the user outage probability can be reduced by introducing flexible relays into the system [7]. However, the EUTRA-based technology solution on the user equipment (UE)-to-network relay presented in Release-13 is insuffi-

cient, which is not the case for fifth-generation (5G) mobile communications and future systems [2].

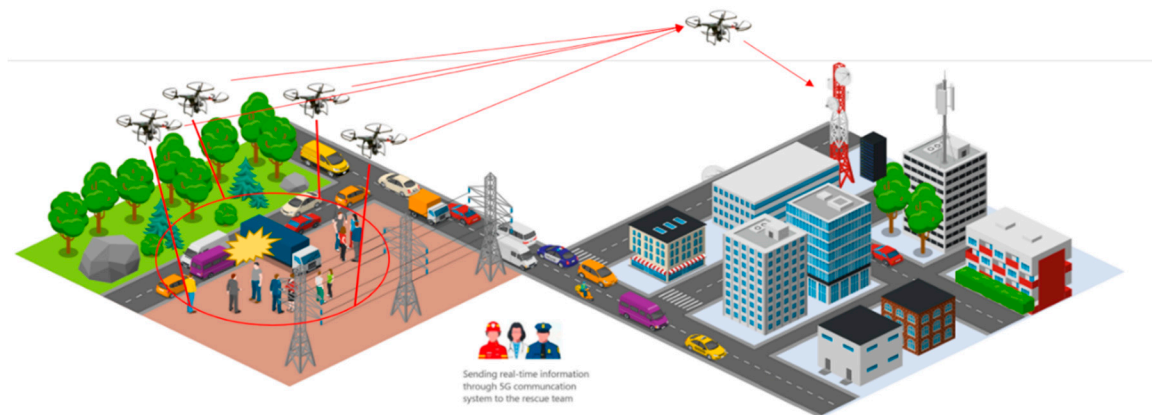


Figure 1. Relaying UAV scenario.

Relay UAVs are studied in several aspects: fixed and mobile UAV relay applications [8–10], energy-efficient trajectories, power and resource optimization [3,11–14], multihop Single and Dual Link options [15–17], and methods to define the number of drones needed to provide connectivity during life-threatening Scenarios [15,17]. Although it is still not possible to find a solution for every problem, the aforementioned issues are interdependent and are often collectively considered designs for heterogeneous networks (HetNets).

Mobile relays are potentially more adaptable to environmental dynamics in future networks due to their ability to be closer to the ground node that needs communication support and, consequently, improves overall throughput.

Most of the solutions in the literature about trajectory optimization propose both successive convex approximation (SCA) and an iterative algorithm as suboptimal solutions to a non-convex problem. Usually, the trajectory specifications (i.e., initial position, speed, route, altitudes, and direction) are associated with radio resource management parameters such as bandwidth, throughput, power allocation, channel variation, outage probability, timeslots, and latency. Energy efficiency and reliability are common constraints due to UAV power source limitations in emergency circumstances.

The most frequent relaying UAV algorithms are amplify and forward (AF) and decode and forward (DF). Chen [15] evaluates the utilization of single-hopping and dual-multihopping cases. The author concludes that the dual-hop multi-link option is better than the multi-hop single link option when air-to-ground path loss parameters depend on UAV positions. The researcher also concludes that decode-and-forward UAVs provide better performances than amplify-and-forward UAVs.

The multihopping problem is considered a nonconvex problem by Zhang et al. [16] and Liu [17]. Zhang proposes an iterative algorithm to obtain a suboptimal solution that maximizes the end-to-end throughput as it is seen in the trajectory optimization problem previously. The difference, in this case, includes parameters to avoid collision and to control average/peak transmission power in the source and the UAV relays. Liu discovers that device-to-device communication (D2D) can be applied to extend coverage to overcome energy limitations on UE. Liu also suggests a shortest-path-routing algorithm to define the minimum number of connections required to minimize the outage probability and the number of hops to support all users.

D2D communication is a feature included in next-generation telecommunication systems because it provides extended coverage, energy efficiency, reduced backhaul demands, low latency with reduced transmission delays, and is considered a key method for achieving green communications. IEEE 802.11a, the wireless local area network, Infrared, and

near field communications implement D2D communication. All these applications operate on an unlicensed spectrum and they are limited by device proximity [18].

Relay-assisted D2D communication is a promising technology that can be deployed in future wireless communications that may improve its spectrum efficiency and coverage area on a licensed spectrum [17].

Ban and Jung present studies where all device members share the same frequency band in the network. However, to prevent mutual interference, the base station (BS) reserves a dedicated radio resource for D2D communication and proposes both a centralized and a distributed scheduling algorithm [19]. Zhou et al. [20] consider that interference cancelation combined with a power optimization algorithm minimizes the intracell and intercell interference in HetNets. Mao et al. [21] research the transmission rate through cooperation. According to the author, next-generation devices will have information regarding neighboring conditions, and the wireless channel and position information will be essential to establish cooperation schemes. Cheng et al. [22] integrate mobile with D2D communication networks, which is used to deliver delay-tolerant packets using store-carry-forward techniques.

A UAV extends proximity services as a D2D device while being used as a surveillance tool ensuring safety and efficient connections between cars as reported by [5].

In Liu et al.'s experiment [23], UAVs assist D2D users while flying under a mission (i.e., deliver a packet, monitoring traffic, etc.) The author states, it is possible to upload messages when the drone approaches the users and sends the messages to the core when the drone is near a base station. The experiment considers UAV selection, time allocation of data loading and offloading, as well as channel access competition. In [17], D2D is applied to extend coverage through multihopping techniques where a partial coverage user connects to an out-of-coverage user in such a way that the relaying links are optimized.

The management control of UAVs can be integrated using software-defined networks (SDN), container-based network function virtualization (NFV), or fog computing architectures where each drone sends information regarding battery status and location to provide replacement if it is necessary and, at the same time, avoid physical collision with other drones in the network improving scalability and efficiency [24].

This paper shows how speed affects overall transmission using multiantenna relaying drones in public safety emergencies. Our scenario implements a circular trajectory and estimates the sum of the data rates delivered to users in a network using MIMO sidelinks. In this section, we review the evolution of sidelink implementation from Release 12 to Release 17, the procedure to establish sidelinks communication, and MIMO basic concepts. The system model is introduced in Section 2, followed by the results in Section 3, and the conclusion and some topics for future work are presented in Sections 4 and 5, respectively.

1.1. Sidelink Communications

One communication tool that is possibly applicable in public safety scenarios is the new radio sidelink (SL), a device to device (D2D) protocol introduced in the 3GPP Release 16 [25] that assists vehicle to everything communications (V2X) and provides road safety services under the Ultra-Reliable low latency communications paradigm (URLLC). The architecture supports both out-of-coverage and in-network coverage situations for broadcast, groupcast, and unicast communications, as presented in Figure 2.

The idea of D2D communication in public safety scenarios is not new. In Fact, Release 12 presents a feature that supports communication when the base station malfunctions or is the target of cyber-attacks [26]. Release 12 prioritizes the issues of implementing broadcast communication where there is no channel state information (CSI) and reception acknowledgment in D2D protocols. Furthermore, according to Lien et al. [27], in Release 12, SL communication has synchronization issues, i.e., UE nodes that are not, allocated inside the D2D network should not send time reference signals, but they do and the opposite is also true, i.e., UE nodes inside the network should send time reference signals, but they

don't. Another problem is that the SL protocol is enabled in the UE even though there are no other devices to communicate.

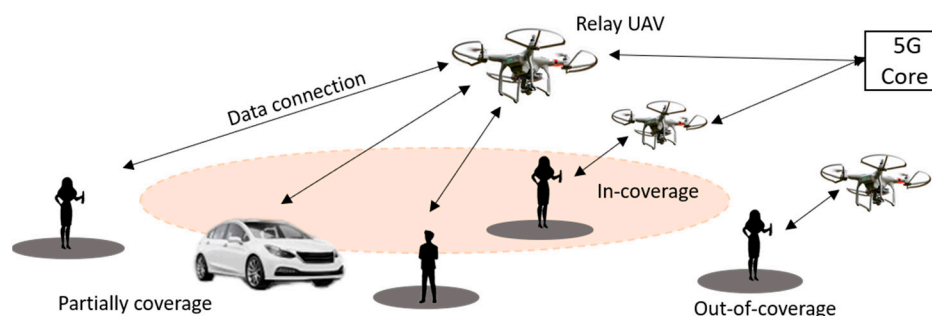


Figure 2. Public safety scenarios available in device to device communication using UAVs.

In Release 13, SL incorporates a Layer 3 (network) feature that extends coverage called the UE-to-Network relay. The main objective is connecting out-of-coverage UEs to the LTE evolved NodeBs (eNB) through the in-coverage UE. The integration with V2X scenarios in Release 14, introduces CSI and improves the physical sidelink control channel (PSCCH) multiplex schemes because of the low latency and a large amount of connection requirements.

Release 15 adds carrier aggregation, transmission diversity to reduce delay, and increases the capacity of the network. The concept of scheduling in the UE was introduced and Release 16 prioritized use cases related to car communication [28].

In the next Release 17 [29], SL relaying features will be studied, including user equipment (UE)-to-network relay for network coverage extension. The physical sidelink feedback channel (PSFCH) will be incorporated to inform the transmitting status of the UE. Besides, the UAV communication will be incorporated in the standard, and there are some discussions on introducing public safety and gaming scenarios in D2D communications.

1.2. Communication Procedure Using Sidelinks

D2D is established using the PC5 interface. The basic procedure to connect elements in the network is performed in three steps: Discovery, Synchronization, and Communication. Discovery includes the steps for finding UEs and non-user devices. The protocol stack includes MAC and PHY layers and uses the sidelink reference signal received power (S_RSRP) in all subchannels to select the relay UAV available to establish the connection.

Synchronization refers to the protocol message exchange and connection configuration. Both control signals that configure sidelink identification are the primary and secondary sidelink synchronization signals (PSSS) and (SSSS), respectively, in frequency and time known as the sidelink synchronization signals (SLSS) and the master information block-sidelink (MIB-SL), which is used for information. A header field in the SLSS signal (SLSS ID) at the receiver UE identifies a connection between the transmitter and the relay in LTE.

The synchronization requirement relationship is described in Equation (1).

$$S_RSRP - MinSrsrp > syncRef_{thres} \quad (1)$$

where the S_RSRP is the sidelink reference signal received power measured, $MinSrsrp$ is the minimal signal power configured in the UE and $syncRef_{thres}$ is the preconfigured threshold available and the relay and in the UE.

This procedure is necessary because both UEs are not connected together and the receiving UE needs information from the MIB (e.g., sl-bandwidth, in-coverage status, directFrameNumber). The strongest S_RSRP is selected as the $syncRef_{thres}$ UE. Sender synchronization is required when the resource pool associated with transmission (Tx) is not from a neighboring cell or from an in-coverage UE. UAV usability provides the reference signal to other devices by taking advantage of the line-of-sight (LoS) UAV characteristics.

1.3. UAV in D2D Communication Using MIMO

UAVs add a degree of complexity to sidelink communications due to the joint UAV mobility control and communication resource allocation problem, the unique channel of UAV-ground links, and the possible doppler effects related to speed differences between cars and UAVs. Massive multiple-input-multiple-output (mMIMO) technology is the next feature to be standardized. In Release 16, only a 2×2 in 2 layers is mentioned to enhance system performance [27] and mMIMO can exploit array gain, spatial multiplexing, and channel reciprocity to provide communication using sidelink protocols in UAVs [30]. Geraci et al. [31] compares mMIMO in single-user and multi-user scenarios. Sboui et al. [32] describe achieving the throughput in relay systems by only increasing power. Feng [33], uses MIMO techniques to estimate the channel between UAVs and internet of Things (IoT) devices. Communication constraint studies, such as Shaik et al. [18], suggest that the implementation of MIMO technology in D2D relay systems improves power management through energy harvesting techniques. The author analyzes outage probability and throughput.

Two well-known MIMO techniques related to diversity and spatial multiplexing are the Alamouti [34] and zero-forcing (ZF) algorithms [35], respectively. The Alamouti (2×2) provides a second-order diversity advantage and the message is decoded with a simple algorithm [36]. In this case, the operation $*$ represents the complex conjugate, the receiver signal y_1 and y_2 can be expressed as:

$$\begin{cases} y_1 = h_1 c_1 + h_2 c_2 + n_1 \\ y_2 = -h_1 c_2^* + h_2 c_1^* + n_2 \end{cases} \quad (2)$$

where h_1 and h_2 represent the channel while n_1 and n_2 are the complex random variables related to noise and interference and c_1 and c_2 are the transmitted signal from the first and second antenna respectively.

In the zero-forcing algorithm, the receiver signal y (Equation (3)) is combined linearly and it can be expressed as a composition of the signal transmitted s and precoded using the Zero forcing-ZF technique, the transmit filter P , the channel H , and, the noise n are received at several receivers. G is the receiver filter with is unitary. In this case, the operation $*$ represents convolution.

$$y = H * P * G * s + n \in \mathbb{C} \quad (3)$$

where P is given by:

$$P = H' * (H * H')^{-1} \quad (4)$$

Both techniques are compared in the NS3 LTE physical layer, where the simulator granularity is the resource block.

2. System Model

The UAV-enabled network presented in Figure 3 where $R = \{r_1, \dots, r_m, \dots, r_M\}$ relaying UAV (usually identified as a drone) distributed on the edges of several concentric circles with a radius of 15–80 m, and heights starting at 20 m–30 m respectively, to avoid collisions. The UAVs flew in a circular trajectory with an angular speed of 5 m/s. There were $N = \{1, \dots, n, \dots, N\}$ users concentrated in a $350 \times 200 \text{ m}^2$ region who moved in random directions and at random speeds. The users' height was configured at $z = 1.5 \text{ m}$. The evolved NodeBs (enB) were located at a height of 120 m and positioned at 300 m. This was the maximum height described in the European Union aircraft regulations [37].

The base station was connected to the remote host, which was a representation of the Evolved Packet Core (EPC) that included the Serving Gateway-SGW-Packet Data Network Gateway PGW, Mobility Management Entity-MME servers, and the futurist U-Space server. In this experiment, the eNB was not able to send packets directly to the users.

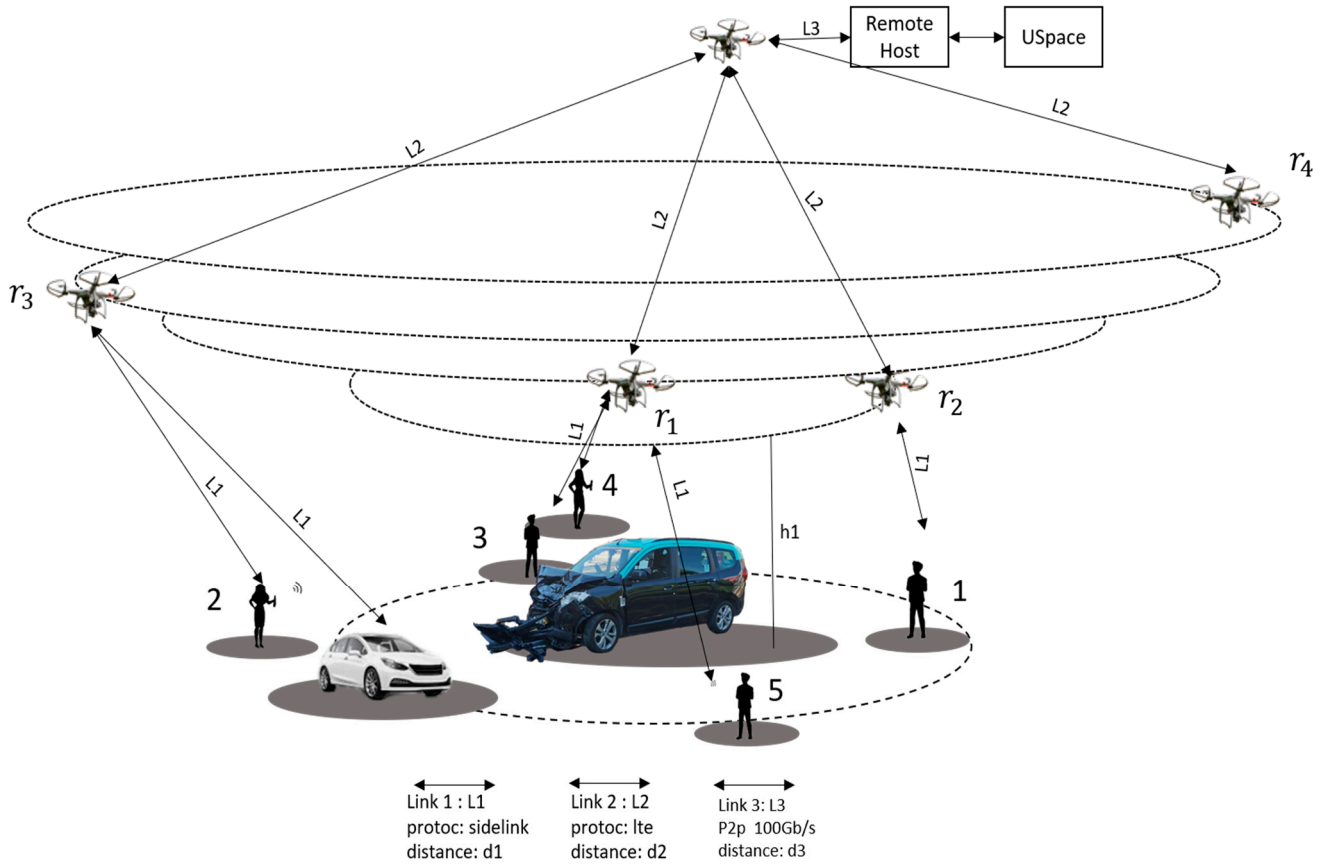


Figure 3. Simulation Scenario. Four relaying drones with circular mobility and speed 5 m/s connecting people to LTE core.

The connection between the remote host, which is responsible for providing internet services to the users was established using three different links. The first one was a sidelink protocol link (L1) provided by the national institute of standards and technology—NIST—, the second used the LTE protocol—(L2), and the last one was simulated as a peer-to-peer connection named L3.

Without loss of generality the Euclidean 3D equation to describe the distance between the base station and the drones as well as the distance between the drones and the users is presented in Equation (5).

$$d_{ru} = \sqrt{(x_r - x_{u_a})^2 + (y_r - y_{u_a})^2 + (z_r - z_{u_a})^2} \quad (5)$$

where (x_r, y_r, z_r) and (x_u, y_u, z_u) are the user and relaying coordinates, respectively.

To test the communication availability in the described scenario we adopted the network simulator 3.31 (NS 3.31) [38] for public safety operations which included the LTE protocol stack for communication and preconfigured sidelink protocols. According to the author [38], the LTE module had a PC5 interface that handled out-of-range scenarios that included data plane and control plane adjustments. In this configuration, we used the IPv6 network protocol. Connections were established according to users' requests and relay services availability using a relay selection algorithm. The search for possible relay services happened every discovery period. The S_RSRP measurements of possible candidates occurred every four discovery periods and the evaluation of candidates occurred every sixteen discovery periods. In the synchronization phase, both devices' exchange pools defined the frequency and bandwidth that were used. The packets were sent to the internet over a dedicated bearer using the LTE uplink configuration for transmission and reception. It used a half-duplex communication. In case of UAV replacement need, the

users were transferred to other available drones using the discovery, synchronization, and communication procedure available in PC5.

The parameters used to configure the experiment are presented in Table 1. The frequency range chosen was a part of the 5G sub 6 GHz bands, which was band 22–35 GHz. According to the 3GPP [39], the maximum number of connections using D2D communication is 16 due to resource management configurations. The implementation of MIMO features in the simulator was an abstraction of the perceived gain in the receiver when compared to SISO systems and it did not include the math needed to compute antenna correlation. Consequently, there was no degradation model related to the path correlation estimate in this experiment. This experiment used two MIMO techniques including Tx Diversity and the Spatial Multiplex Open Loop. The maximum drone speed limit was 160 km/h [40].

Table 1. Frequencies bands used in the simulation.

| General Parameters | Values |
|--------------------------|--------|
| Relay UAV Height [m] | 20–30 |
| eNB Height [m] | 120 |
| Relay drone radius [m] | 20–400 |
| Relay Speed [m/s] | 5 |
| User's height [m] | 1.5 |
| Uplink Frequency [MHz] | 3410 |
| Downlink Frequency [MHz] | 3510 |
| Bandwidth [MHz] | 50 |
| Relay Power [dBm] | 20 |
| Users Power [dBm] | 20 |
| eNB Power [dBm] | 40 |
| Simulation Time [s] | 100 |

3. Results

Figure 4 shows the allocated positions for users and the relaying UAV during the experiment. The figure highlights the drones' relay, the users' initial and final positions, and the number of users in the simulation. The base station is not represented in the figure but is located 300 m from the relays, as described in the previous section. In the simulation, UAVs establish a relay connection with nearby users and send their data to a remote host, as illustrated in Figure 3. The UAVs move in concentric circles at a radius of 20, 50, and 80 m. Meanwhile, the users move randomly according to the Random Walk principle. The network uses the round-robin (RR) scheduler. The network's topology and dynamics infer that the modulation and coding schemes may adapt according to the channel phenomena (distance, interference, fading, etc.) received in the channel quality indicator (CQI) parameter. The overall throughput is estimated considering the number of relays, bandwidth, number of resource blocks available, and the transmission time interval in LTE [36].

Figure 5 illustrates the percentage of received packets as a function of the relaying UAV's speed. In this experiment, three relaying UAVs are used to establish communication with the user groups allocated to each UAV. For example, UAV 1 supports 4 users, then UAV 2 supports 4 additional users, etc. There are three group scenarios in this simulation, i.e., 4 users, 5 users, and 6 users.

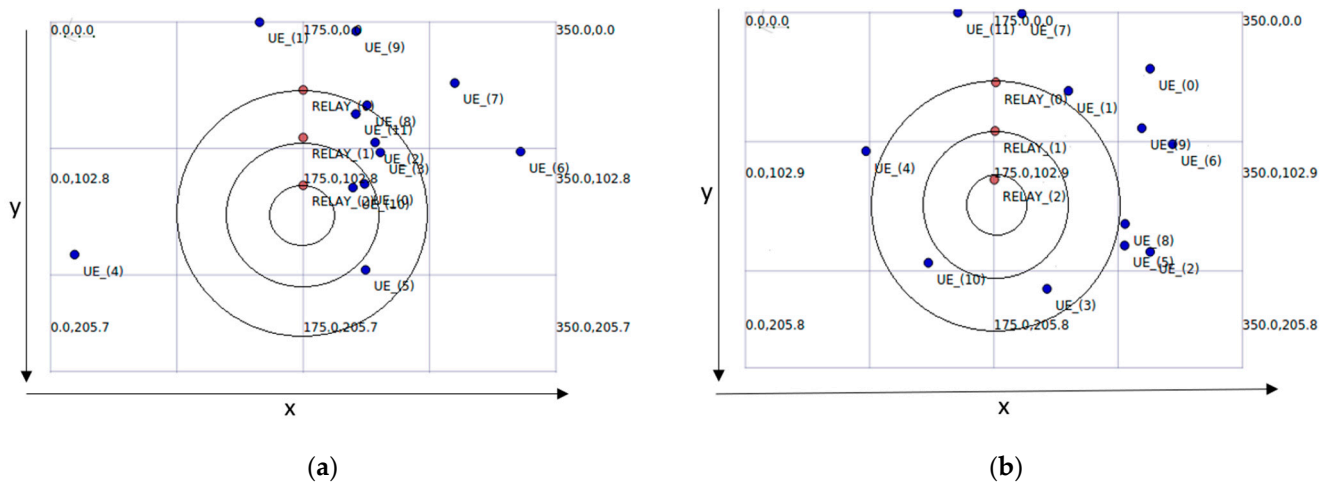


Figure 4. Users and relaying UAVs positions in the simulated scenario: (a) In blue: users’ initial position. In brown: relay UAVs initial position; (b) In blue: users’ final position. In brown: relay final position inside $350 \times 200 \text{ m}^2$ area.

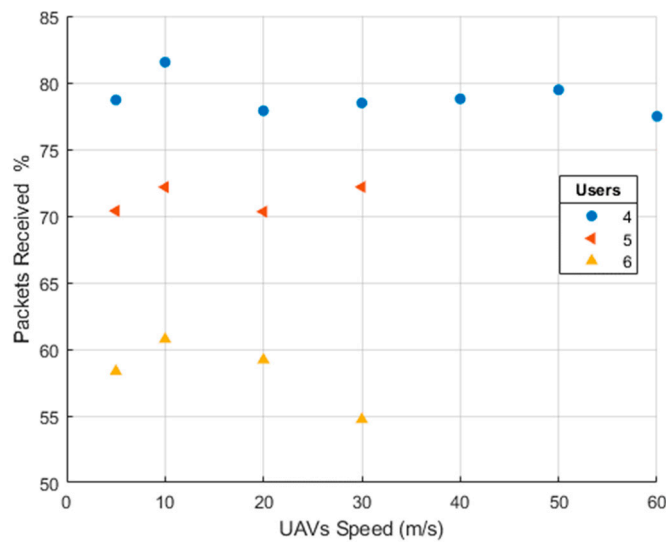


Figure 5. Effects of speed on the overall throughput per users’ groups. Relaying drone = 3. MIMO technique: Alamouti.

The overall throughput exhibits the same behavior. The only exception is group 3, which has 6 users, where the overall packet reception decreases at a speed of 30 m/s instead of increases when compared to its measurements at 20 m/s. The peak that occurs at 10m/s may be related to the physical layer configuration changes that support quick communication. These changes are based on the adaptative modulation and coding schemes that support the simulation and the reserve resource blocks for PSCCH/PSSCH signals for retransmissions. Some improvements might be justified using group communication techniques.

Figure 6 presents the effect of increasing the number of UAVs in the network. In this simulation, the number of relaying drones is increased while the number of users per relaying UAV and the speed is fixed at 4 and 10 m/s, respectively. As a relay is included in the network, the number of connected users also increases, and the overall packet reception is affected by that. In this study, we do not consider the D2D connection between users.

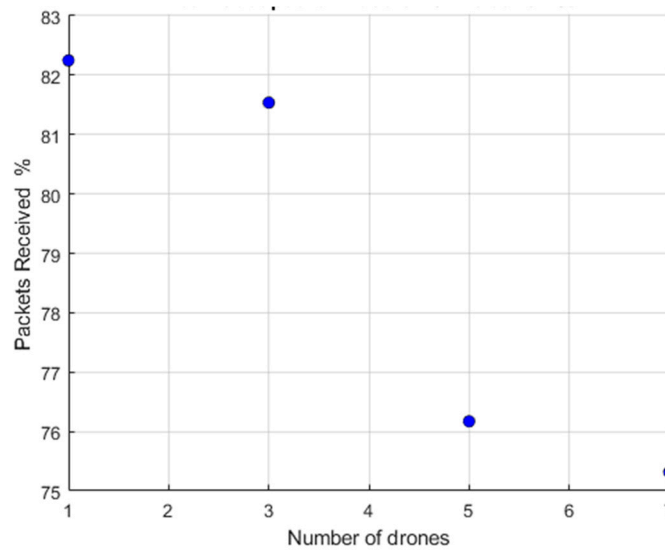


Figure 6. Effects of increasing the number of drones; users = 4, speed = 10 m/s MIMO technique: Alamouti.

Figure 7 compares MIMO techniques when the speed is configured to 10 m/s, and the number of users is 4 and 8, respectively. Despite the gain diversity and spatial multiplexing included in the NS3 algorithm, no effect is observed in relation to the SISO system.

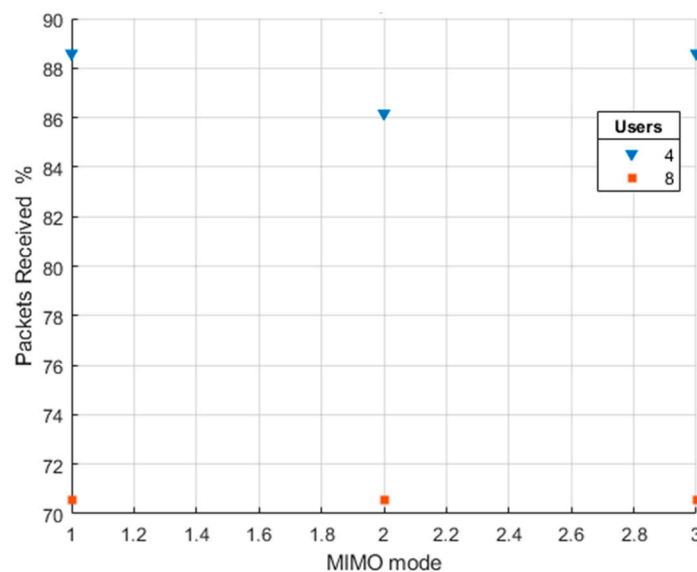


Figure 7. MIMO techniques: 1—SISO; 2—Alamouti; 3— 2×2 MIMO ZF.

Despite the diversity gain and the spatial multiplexing included in MIMO [41], which provides a one or two-layer gain as defined in [39], in the simulation with 4 users, the throughput was reduced, and the one with 8 users kept constant. These results may be explained by distance and channel modeling between both links: eNB—relay and relay—user.

4. Conclusions

This work mainly shows the simulation of communication performance supported by UAVs relay using circular movement as a mobility model in NS3 simulator to analyze the impact on UAV relay serving users in unfortunate circumstances using sidelink protocol.

We conclude that some relevant parameters to be considered when developing drones for communication that use sidelink protocols are one speed and the number of users that need the connection simultaneously.

With fewer user connections (i.e., three) it is possible to maintain approximately 80% of the packet reception rate at 60 m/s (equivalent to 216 km/h). As the speed and the number of users is increased, the network quality decreased proportionately down to 55% packet reception at 30 m/s with 6 connected users.

Furthermore, the number of relaying UAVs in the network reduced the overall transmission rate. The packet reception dropped to nearly 75% after adding seven relaying drones to the network in our scenario. However, the results presented in both figures show that it is better to add more relaying UAVs than to increase the number of connections in one UAV to achieve the desired quality of services (QoS) requirements.

Regarding MIMO techniques tested, a clear indication that using MIMO will improve the overall transport block transmission was not observed.

5. Future Work

In future work, we plan to integrate sidelink relay communication in the new radio communication system 5G and test new mobility models to improve QoS requirements and energy efficiency.

Author Contributions: Conceptualization, J.V.; Investigation, J.V.; software, J.V.; supervision, F.C. and P.S.; validation, A.C. and R.D.; writing, original draft, J.V.; writing, review and editing, F.C., P.S., A.C. and R.D. All authors have read and agreed to the published version of the manuscript.

Funding: This research received funding from the European Union's Horizon 2020 research and innovation program under the Marie Skłodowska-Curie Project Number 813391 and Fundação para a Ciência e Tecnologia and Instituto de Telecomunicações under project UIDB/50008/2020.

Data Availability Statement: The data presented in this study are available on request from the corresponding author. The data are not publicly in this study due to project restrictions

Acknowledgments: The authors would like to express their great appreciation to the Drones journal Editors and anonymous Reviewers for their valuable suggestions, which improved the manuscript quality.

Conflicts of Interest: The authors declare no conflict of interest.

References

1. Release 15—Technical Specification Group Radio Access Network. Available online: <https://www.3gpp.org/release-15> (accessed on 14 March 2021).
2. Kaleem, Z.; Yousaf, M.; Qamar, A.; Ahmad, A.; Duong, T.Q.; Choi, W.; Jamalipour, A. UAV-Empowered Disaster-Resilient Edge Architecture for Delay-Sensitive Communication. *IEEE Netw.* **2019**, *33*, 124–132. [[CrossRef](#)]
3. Chen, Q. Joint Trajectory and Resource Optimization for UAV-Enabled Relaying Systems. *IEEE Access* **2020**, *8*, 24108–24119. [[CrossRef](#)]
4. Sesar—Joint Undertaking, “U-Space”. 2018. Available online: <https://www.sesarju.eu/U-space> (accessed on 10 September 2020).
5. Bekkouche, O.; Samdanis, K.; Bagaa, M.; Taleb, T. A Service-Based Architecture for Enabling UAV Enhanced Network Services. *IEEE Netw.* **2020**, *34*, 328–335. [[CrossRef](#)]
6. Hiraguri, T.; Nishimori, K.; Shitara, I.; Mitsui, T.; Shindo, T.; Kimura, T.; Matsuda, T.; Yoshino, H. A Cooperative Transmission Scheme in Drone-Based Networks. *IEEE Trans. Veh. Technol.* **2020**, *69*, 2905–2914. [[CrossRef](#)]
7. Fu, J.; Wu, G.; Li, R. Performance Analysis of Sidelink Relay in SCMA-Based Multicasting for Platooning in V2X. In Proceedings of the 2020 IEEE International Conference on Communications Workshops (ICC Workshops), Dublin, Ireland, 7–11 June 2020.
8. Zhang, J.; Zeng, Y.; Zhang, R. Spectrum and energy efficiency maximization in UAV-enabled mobile relaying. In Proceedings of the 2017 IEEE International Conference on Communications (ICC), Paris, France, 21–25 May 2017; pp. 1–6. [[CrossRef](#)]
9. Wang, L.; Hu, B.; Chen, S.; Cui, J. UAV-Enabled Reliable Mobile Relaying Based on Downlink NOMA. *IEEE Access* **2020**, *8*, 25237–25248. [[CrossRef](#)]
10. Song, Q.; Zheng, F. Energy efficient multi-antenna UAV-enabled mobile relay. *China Commun.* **2018**, *15*, 41–50. [[CrossRef](#)]
11. Jiang, X.; Wu, Z.; Yin, Z.; Yang, Z. Power and Trajectory Optimization for UAV-Enabled Amplify-and-Forward Relay Networks. *IEEE Access* **2018**, *6*, 48688–48696. [[CrossRef](#)]

12. Zeng, S.; Zhang, H.; Bian, K.; Song, L. UAV Relaying: Power Allocation and Trajectory Optimization Using Decode-and-Forward Protocol. In Proceedings of the 2018 IEEE International Conference on Communications Workshops (ICC Workshops), Kansas City, MO, USA, 20–24 May 2018; pp. 1–6.
13. Zhang, T.; Liu, G.; Zhang, H.; Kang, W.; Karagiannidis, G.K.; Nallanathan, A. Energy-Efficient Resource Allocation and Trajectory Design for UAV Relaying Systems. *IEEE Trans. Commun.* **2020**, *68*, 6483–6498. [[CrossRef](#)]
14. Song, K.; Zhang, J.; Ji, Z.; Jiang, J.; Li, C. Energy-Efficiency for IoT System with Cache-Enabled Fixed-Wing UAV Relay. *IEEE Access* **2020**, *8*, 117503–117512. [[CrossRef](#)]
15. Chen, Y.; Zhao, N.; Ding, Z.; Alouini, M.-S. Multiple UAVs as Relays: Multi-Hop Single Link Versus Multiple Dual-Hop Links. *IEEE Trans. Wirel. Commun.* **2018**, *17*, 6348–6359. [[CrossRef](#)]
16. Zhang, G.; Yan, H.; Zeng, Y.; Cui, M.; Liu, Y. Trajectory Optimization and Power Allocation for Multi-Hop UAV Relaying Communications. *IEEE Access* **2018**, *6*, 48566–48576. [[CrossRef](#)]
17. Liu, X.; Li, Z.; Zhao, N.; Meng, W.; Gui, G.; Chen, Y.; Adachi, F. Transceiver Design and Multihop D2D for UAV IoT Coverage in Disasters. *IEEE Internet Things J.* **2019**, *6*, 1803–1815. [[CrossRef](#)]
18. Shaik, P.; Singya, P.K.; Kumar, N.; Garg, K.K.; Bhatia, V. On Impact of Imperfect CSI over SWIPT Device-to-Device (D2D) MIMO Relay Systems. In Proceedings of the 2020 International Conference on Signal Processing and Communications (SPCOM), Bangalore, India, 19–24 July 2020. [[CrossRef](#)]
19. Ban, T.-W.; Jung, B.C. On the Link Scheduling for Cellular-Aided Device-to-Device Networks. *IEEE Trans. Veh. Technol.* **2016**, *65*, 9404–9409. [[CrossRef](#)]
20. Zhou, Z.; Dong, M.; Ota, K.; Wang, G.; Yang, L.T. Energy-Efficient Resource Allocation for D2D Communications Underlying Cloud-RAN-Based LTE-A Networks. *IEEE Internet Things J.* **2016**, *3*, 428–438. [[CrossRef](#)]
21. Mao, H.; Feng, W.; Ge, N. Performance of Social-Position Relationships Based Cooperation among Mobile Terminals. *IEEE Trans. Veh. Technol.* **2016**, *65*, 3128–3138. [[CrossRef](#)]
22. Cheng, N.; Lu, N.; Zhang, N.; Yang, T.; Shen, X.; Mark, J.W. Vehicle-assisted device-to-device data delivery for smart grid. *IEEE Trans. Veh. Technol.* **2016**, *65*, 2325–2340. [[CrossRef](#)]
23. Liu, D.; Xu, Y.; Wang, J.; Chen, J.; Wu, Q.; Anpalagan, A.; Xu, K.; Zhang, Y. Opportunistic Utilization of Dynamic Multi-UAV in Device-to-Device Communication Networks. *IEEE Trans. Cogn. Commun. Netw.* **2020**, *6*, 1069–1083. [[CrossRef](#)]
24. Pinto, M.F.; Marcato, A.L.M.; Melo, A.G.; Honório, L.M.; Urdiales, C. A Framework for Analyzing Fog-Cloud Computing Cooperation Applied to Information Processing of UAVs. *Wirel. Commun. Mob. Comput.* **2019**, *2019*, 7497924. [[CrossRef](#)]
25. Release 16—3GPP—Technical Specification Group Radio Access Network, NR; NR and NG-RAN Overall Description—Stage 2—TS 38.300 version 16.2.0. Available online: <https://www.3gpp.org/release-16> (accessed on 10 September 2020).
26. Lien, S.-Y.; Chien, C.-C.; Tseng, F.-M.; Ho, T.-C. 3GPP device-to-device communications for beyond 4G cellular networks. *IEEE Commun. Mag.* **2016**, *54*, 29–35. [[CrossRef](#)]
27. Lien, S.-Y.; Deng, D.-J.; Lin, C.-C.; Tsai, H.-L.; Chen, T.; Guo, C.; Cheng, S.-M. 3GPP NR Sidelink Transmissions Toward 5G V2X. *IEEE Access* **2020**, *8*, 35368–35382. [[CrossRef](#)]
28. Rouil, R.; Cintrón, F.; Mosbah, A.B.; Quintiliani, S.G. A Long Term Evolution (LTE) device-to-device module for ns-3. In Proceedings of the Workshop on ns-3 (WNS3), Seattle, WA, USA, 15–16 June 2016; pp. 3–5. Available online: https://www.nsnam.org/workshops/wns3-2016/posters/wns3_2016_LTE_D2D_NIST.pdf (accessed on 10 September 2020).
29. Release 17—Technical Specification Group Radio Access Network. Available online: <https://www.3gpp.org/release-17> (accessed on 14 March 2021).
30. Chandhar, P.; Larsson, E.G. Massive MIMO for Connectivity with Drones: Case Studies and Future Directions. *IEEE Access* **2019**, *7*, 94676–94691. [[CrossRef](#)]
31. Geraci, G.; Garcia-Rodriguez, A.; Giordano, L.G.; Lopez-Perez, D.; Bjoernson, E. Supporting UAV Cellular Communications through Massive MIMO. In Proceedings of the 2018 IEEE International Conference on Communications Workshops (ICC Workshops), Kansas City, MO, USA, 20–24 May 2018; pp. 1–6.
32. Sboui, L.; Ghazzai, H.; Rezk, Z.; Alouini, M.-S. Achievable Rates of UAV-Relayed Cooperative Cognitive Radio MIMO Systems. *IEEE Access* **2017**, *5*, 5190–5204. [[CrossRef](#)]
33. Feng, W.; Wang, J.; Chen, Y.; Wang, X.; Ge, N.; Lu, J. UAV-Aided MIMO Communications for 5G Internet of Things. *IEEE Internet Things J.* **2019**, *6*, 1731–1740. [[CrossRef](#)]
34. Alamouti, S.M. A simple transmit diversity technique for wireless communications. *IEEE J. Sel. Areas Commun.* **1998**, *16*, 1451–1458. [[CrossRef](#)]
35. Joham, M.; Utschick, W.; Nossek, J. Linear transmit processing in MIMO communications systems. *IEEE Trans. Signal Process.* **2005**, *53*, 2700–2712. [[CrossRef](#)]
36. Shah, V.K.; Gharge, A.P. A Review on Relay Selection Techniques in Cooperative Communication. *Int. J. Eng. Innov. Technol.* **2012**, *2*, 65–69. Available online: https://pdfs.semanticscholar.org/32cc/eb958904ac97356a7eef56c583795969f5a5.pdf%0Ahttp://ijeit.com/vol2/Issue5/IJEIT1412201211_12.pdf (accessed on 10 January 2020).
37. Easy Access Rules for Unmanned Aircraft Systems (Regulation (EU) 2019/947 and Regulation (EU) 2019/945). Available online: <https://www.easa.europa.eu/document-library/easy-access-rules/easy-access-rules-unmanned-aircraft-systems-regulation-eu> (accessed on 10 January 2021).
38. Network Simulator 3 (NS3) Documentation. Available online: <https://www.nsnam.org/> (accessed on 10 September 2020).

-
39. 3Gpp—A Global Initiative—The Mobile Broadband Standard. Available online: <https://www.3gpp.org/> (accessed on 10 November 2020).
 40. Federal Aviation Administration. Commercial Operators Certification. Available online: https://www.faa.gov/uas/commercial_operators/ (accessed on 10 November 2020).
 41. 3GPP—A Global Initiative, Technical Specification—LTE; Evolved Universal Terrestrial Radio Access (E-UTRA); Physical Layer Procedures (3GPP TS 36.213 version 13.0.0 Release 13). 2017. Available online: https://www.etsi.org/deliver/etsi_ts/136200_136299/136213/14.02.00_60/ts_136213v140200p.pdf (accessed on 10 January 2021).